BeamWarrior —advanced optical analysis for integrated modeling

Rainer Wilhelm[a], Bertrand Koehler[a], Ulrich Johann[b], Michael Kersten[b], Raphael Schwarz[b]
[a]European Southern Observatory (ESO), Garching b. München, Germany[¶]
[b]Astrium GmbH, Friedrichshafen, Germany

ABSTRACT

As part of an "Integrated Modeling Toolbox" described in *Wilhelm, Koehler et al. 2002* (these proceedings)[11] the optical modeling tool **BeamWarrior** has been developed. Its main purpose is the creation of optical models for integration into a dynamic control system simulation. Offering a versatile set of geometrical and wave optical propagation algorithms it can also be used for sophisticated static optical analysis. The article summarizes the functional features of the tool and describes its algorithms —both, from a theoretical and practical point of view.

Keywords: integrated modeling, geometrical optics, ray tracing, physical optics, diffraction, wave propagation, beam decomposition, Gaussian beam

1. INTRODUCTION

In a joint effort, ESO, Astrium GmbH and the Institute for Lightweight Structures, Technical University of Munich are developing a software package for "integrated modeling" of single- and multi-aperture optical telescopes. Integrated modeling aims at time-dependent system analysis combining different technical disciplines (optics, mechanical structure, control system with sensors and actuators). Different environmental and internal disturbances can be taken into account. Main applications of integrated modeling are feasibility assessment and performance prediction. The architecture of the software package with its tools **SMI** and **BeamWarrior** is described in *Wilhelm, Koehler et al. 2002* (these proceedings).[11] This article focuses on the core of the optical modeling tool **BeamWarrior**: the "Kernel" with its beam propagation algorithms. Section 2 summarizes the functionality of the Kernel. A detailed description of the algorithms for modeling light propagation is given in Section 3. Finally, Section 4 discusses advantages and drawbacks of the individual beam propagation algorithms regarding their application in practice.

2. THE BeamWarrior KERNEL

BeamWarrior is used to generate models of the optical signal flow for integration into a dynamic control system simulation based on Matlab / Simulink®. Its development has been initiated in February 1997 driven by the non-availability of a powerful, open-architecture optical modeling code which can be customized to create optical models for integration into a dynamic simulation environment. Present and future development is jointly done by ESO and Astrium GmbH.

¶ Email: rwilhelm@eso.org, World Wide Web: http://www.eso.org/projects/vlti

The **BeamWarrior** *Kernel* forms the core of the tool. It is a library of ANSI C functions for optical modeling which can either be accessed by a user-written customized C application or via the **BeamWarrior** *Optical Modeling Tool*. The latter is generic-purpose application reading the sequence of computational steps to be performed and the results to be produced from an ASCII "control file". The Optical Modeling Tool has been designed for flexible generation of linear optical models (i.e., sensitivity matrices).[11] Besides its main purpose, namely the creation of dynamic optical models, **BeamWarrior** can also be employed for a large variety of static optical analysis tasks. Examples can be found in the references.[7, 8, 9, 10]

The main functional features of the **BeamWarrior** Kernel are:

- ❏ Optical system definition:
  - — Mathematical surface shapes: (cylindrical) conicoid (flat, spherical, parabolic, elliptic, hyperbolic)
  - — Optical surface types: dielectric (reflecting or refracting), obscuration masks, beam splitters
  - — Usage of global coordinate system (= global coordinate system of a Finite Element structure model)
  - — User defined material catalogue for refractive indices
- ❏ Light propagation on different sequential paths through the optical system
- ❏ Two types of incident beams: homogeneous plane wave, Gaussian TEM_{00}
- ❏ Perturbation of surfaces and incident wavefronts in all degrees of freedom
- ❏ Beam propagation:
  - — Fast and accurate ray tracing for geometrical optical analysis (see Section 3.1)
  - — Three alternative methods for calculating wave optical propagations (see Section 3.2)
  - — All algorithms consider radiometry and polarization
- ❏ Interferometric superposition of optical fields
- ❏ Analysis functions:
  - — Spot diagram
  - — 2-D maps of optical path (difference), electric field amplitude and phase, intensity
  - — Polarization map (2-D map showing the local state of polarization)
  - — Zernike decomposition of wavefronts
  - — Aperture stop and pupil finder
  - — 3-D view of optical system and beam trains

3. BEAM PROPAGATION ALGORITHMS

The assumption of a lossless, isotropic and homogeneous medium (refractive index n) is common to all propagation algorithms. For a given medium wavelength $\lambda = \lambda_0/n$, the task is to compute solutions of the scalar *Helmholtz wave equation*

$$(\Delta + k^2)\underline{E}_q(\mathbf{r}) = 0 \tag{1}$$

in form of scalar complex amplitudes $\underline{E}_q(\mathbf{r})$ (q = x, y, z) representing the three Cartesian components of the electric vector field. The medium propagation constant k is defined as $k = 2\pi/\lambda$.

3.1 Geometrical optical propagation algorithm

Geometrical optics (GO) considers the limiting case $\lambda \to 0$. The electric vector field locally[¶] behaves as a homogeneous plane transverse electromagnetic (TEM) wave. Substituting the "trial" solution $\underline{\mathbf{E}}_q(\mathbf{r}) = \hat{\underline{\mathbf{E}}}_q(\mathbf{r}) \cdot \exp(-jk_0 \cdot \Im(\mathbf{r}))$ into the Helmholtz equation and regarding the case $\lambda \to 0$ one obtains the *eikonal equation* $(\nabla\Im(\mathbf{r}))^2 = n^2$. The scalar function ("eikonal") $\Im(\mathbf{r})$ is a measure of the optical path. The surfaces $\Im(\mathbf{r}) =$ constant define GO wavefronts. Light rays are defined as orthogonal trajectories to these wavefronts. In the assumed case of a homogeneous medium a light ray has the form of a straight line. With the unit vector $\mathbf{i}$ denoting the direction of the light ray, the eikonal can be written as $\Im(\mathbf{r}) = n\mathbf{i} \bullet \mathbf{r}$. The corresponding GO wave signal is

$$\underline{\mathbf{E}}_q(\mathbf{r}) = \hat{\underline{\mathbf{E}}}_q(\mathbf{r}) \cdot \exp(-jk_0 n\mathbf{i} \bullet \mathbf{r}) = \hat{\underline{\mathbf{E}}}_q(\mathbf{r}) \cdot \exp(-j\mathbf{k} \bullet \mathbf{r}) \quad (q = x, y, z). \tag{2}$$

The electric and magnetic field vectors $\underline{\mathbf{E}}$ and $\underline{\mathbf{H}}$ are mutually perpendicular and parallel to the wavefront. Both are perpendicular to the wave vector $\mathbf{k} = k_0 n\mathbf{i}$. $\underline{\mathbf{E}}$ and $\underline{\mathbf{H}}$ share the same phase. The ratio of their magnitudes is the wave impedance $Z = |\underline{\mathbf{E}}|/|\underline{\mathbf{H}}| = Z_0/n$ with the vacuum wave impedance $Z_0 = (\mu_0/\varepsilon_0)^{1/2} \approx 377\Omega$.

A GO beam is modeled by a grid of light rays each having assigned a 2×1 Jones vector $\underline{\mathbf{J}}$. The vector $\underline{\mathbf{J}}$ holds a pair of complex amplitudes $(\underline{E}_{p1}, \underline{E}_{p2})$ with respect to the two local orthogonal polarization directions $\mathbf{p_1}$ and $\mathbf{p_2}$. The three unit vectors $\mathbf{p_1}$, $\mathbf{p_2}$ and $\mathbf{i}$ form a right-handed orthogonal triad with $\mathbf{p_1} \times \mathbf{p_2} = \mathbf{i}$ (see Figure 1). The amplitude ratio and phase difference of the two components $\underline{E}_{p1}$ and $\underline{E}_{p2}$ determines the local state of polarization. A fast vector-based ray tracing algorithm *(Redding & Breckenridge 1991[6])* propagates the ray grid through the optical system consisting of flat, conicoid or cylindrical conicoid surfaces. Each ray is regarded as a sample of a locally plane TEM wave. Therefore, the effect on its Jones vector for reflection or refraction at an optical surface can be described by Fresnel equations. For computing the calibrated power flux through the system, a computationally efficient algorithm has been developed. By using a triangular grid interconnecting the rays (see Figure 1) the approach allows to compute the electric field distribution on a grid of pixels on an optical surface at the expense of a single-forward ray tracing run. For performing the same task, software codes based on stochastic ray tracing require several ray tracing loops from the light source to the target surface. The change in cross-sectional area of a light tube is taken into account for scaling the local squared field amplitude in accordance with the "intensity law of geometrical optics" $I \cdot A =$ constant with the triangle area A and the local intensity $I = 1/(2Z) \cdot |\underline{\mathbf{E}}(\mathbf{r})|^2$. A detailed description of the radiometric polarization ray tracing algorithm can be found in the references.[9, 7]

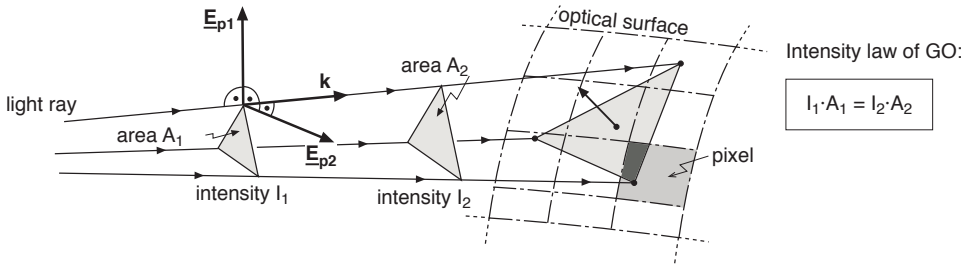

Fig. 1: Triangular ray tubes are used for radiometric scaling of the GO electric field.

¶ The term "locally" means "in a region of the spatial extension of some wavelengths.

3.2 Wave optical propagation algorithms

The limits of validity of the GO model arise from the derivation of the eikonal equation. Practical cases where the GO model is not adequate are the computation of a field distribution close to focus or modeling the propagation of a spatially confined beam over long distances. In these cases, diffraction (i.e. wave optical) effects play an important role. To model such effects, **BeamWarrior** provides a set of different wave optical propagation algorithms which are discussed in the following Subsections 3.2.1, 3.2.2 and 3.2.3. Common to all approaches is their assumption of *scalar diffraction theory*: the coupling of the various vector components of the electric and magnetic field through boundary conditions is neglected. The solution of the Helmholtz equation (Eq. (1)) is computed independently for the three Cartesian components of $\underline{\mathbf{E}}$ resulting in a complete description of the vectorial field. Scalar diffraction theory is an adequate model if (1) apertures are large compared to the wavelength, and (2) a field is not observed too close ($\approx \lambda$) to an aperture.

3.2.1 Direct method

Both, the "direct method" and the "angular spectrum method" (discussed in Subsection 3.2.2) compute the electric field on a "target surface" Σ_t (locations $\mathbf{r_t}$) assuming the knowledge of the electric field on an "object surface" Σ_o (locations $\mathbf{r_o}$). The Helmholtz equation together with the *Kirchhoff boundary condition* for the field on both sides of the aperture on Σ_o and the *Sommerfeld radiation condition* define a boundary value problem.[2] Applying the *Helmholtz–Kirchhoff integral theorem* (derived from *Green's theorem*) with the choice of Sommerfeld's Green's function, one gets the *Rayleigh–Sommerfeld diffraction integral* which forms the base equation of the direct method:

$$\underline{E}_q(\mathbf{r_t}) = \frac{j}{\lambda}\int_{\Sigma_o}\int \underline{E}_q(\mathbf{r_o}) \cdot \frac{\exp(-jk|\mathbf{r_t}-\mathbf{r_o}|)}{|\mathbf{r_t}-\mathbf{r_o}|} \cdot \mathbf{r_{ot}} \bullet \mathbf{n_o} \cdot dS \qquad (q = x, y, z). \tag{3}$$

For implementation on the computer, the integral in Eq. (3) is replaced by a sum. The field on the target surface is computed as a coherent superposition of spherical wave contributions originating at ray positions $\mathbf{r_o}$ on Σ_o. The approach presumes that the grid of ray triangles is known on the object surface Σ_o. Each ray on Σ_o —with its Jones vector— is interpreted as a *Huygens secondary source*. The spherical wave contributions to a pixel at location $\mathbf{r_t}$ are weighted with an "obliquity factor" $\mathbf{r_{ot}} \bullet \mathbf{n_o}$ where $\mathbf{r_{ot}} = |\mathbf{r_t}-\mathbf{r_o}|^{-1} \cdot (\mathbf{r_t}-\mathbf{r_o})$ is the unit vector pointing from $\mathbf{r_o}$ to $\mathbf{r_t}$, and $\mathbf{n_o}$ is the local unit surface normal at the ray location $\mathbf{r_o}$. The surface element dS (which becomes ΔS_o in the sum) associated to the ray at $\mathbf{r_o}$ is derived from the local ray triangle grid structure around $\mathbf{r_o}$. Figure 2 illustrates the principle of the approach.

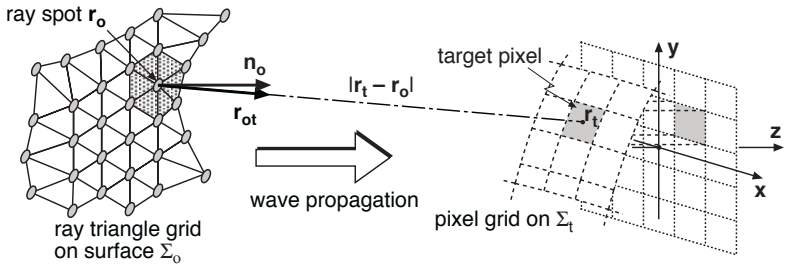

Fig. 2: Principle of the direct method for wave optical propagation

Direct method in paraxial approximation:

The "paraxial approximation" assumes that the field $\underline{E}_q(\mathbf{r}_t)$ can be written as product of a "primary" plane wave propagation factor exp(–jkz) and a wave amplitude $\underline{\Psi}_q(x, y, z)$ whose remaining z-dependence is slow compared to one wavelength and to the transverse variations (along x- and y-direction) due to the finite width of the beam. By dropping the second partial derivative in z, the Helmholtz equation (Eq. (1)) reduces to the paraxial wave equation

$$\frac{\partial^2}{\partial x^2}\underline{\Psi}_q + \frac{\partial^2}{\partial y^2}\underline{\Psi}_q - 2jk\frac{\partial}{\partial z}\underline{\Psi}_q = 0 \qquad (q = x, y, z). \tag{4}$$

Considering the paraxial approximation, the "direct method" solution Eq. (3) becomes

$$\underline{E}_q(x_t, y_t, z_t) = \frac{j}{\lambda z_t} \cdot \exp\left[-jkz_t + \frac{x_t^2 + y_t^2}{2z_t}\right] \cdot \mathcal{F}_{2D}\left\{\underline{E}_q(x_o, y_o, 0) \cdot \exp\left[-jk\frac{x_o^2 + y_o^2}{2z_t}\right]\right\} \qquad (q=x,y,z) \tag{5}$$

with the operator $\mathcal{F}_{2D}$ denoting a two-dimensional Fourier transform $\{x_o, y_o\} \circ\!\!-\!\!\bullet \{f_x, f_y\}$ defined as follows:

$$\mathcal{F}_{2D}\{\Psi(x_o, y_o)\} = \int_{-\infty}^{+\infty}\!\!\int \Psi(x_o, y_o) \cdot \exp[j2\pi(f_x x_o + f_y y_o)]dx_o dy_o\,. \tag{6}$$

The spatial frequencies $\{f_x, f_y\}$ are defined as $f_x = x_t/(\lambda z_t)$ and $f_y = y_t/(\lambda z_t)$. Eq. (5) assumes that the initial field $\underline{E}_q(x_o, y_o, 0)$ is given on a plane Σ_o parallel to the (x, y)-plane and located at z = 0. The diffracted field $\underline{E}_q(x_t, y_t, z_t)$ is computed on a plane Σ_t parallel to Σ_o at a distance $z = z_t$ ("plane-to-plane propagation"). It is proportional to the Fourier transform of the product of the initial field on Σ_o and a "quadratic phase factor" $\exp[-jk(x_o^2 + y_o^2)/(2z_t)]$.

For computing the Fourier transform, **BeamWarrior** makes use of the FFTW library[¶] —a freely available ANSI C library for computing the Fast Fourier Transform (FFT) in one or more dimensions with arbitrary grid size.

3.2.2 Angular spectrum method

A solution to the boundary value problem mentioned in Subsection 3.2.1 is also obtained by superposing all homogeneous and evanescent plane waves traveling in directions **k** whose complex amplitudes are given by the spatial frequency spectrum ("angular spectrum") of the initial field defined in a plane Σ_o:

$$\underline{E}_q(x_t, y_t, z_t) = \int_{\Sigma_o}\!\!\int \mathcal{F}_{2D}\{\underline{E}_q(x_o, y_o, 0)\} \cdot \exp[-j\mathbf{kr}]d\mathbf{k} = \mathcal{F}_{2D}^{-1}\{\mathcal{F}_{2D}\{\underline{E}_q(x_o, y_o, 0)\} \cdot H(f_x, f_y, z_t)\} \tag{7}$$

with the *transfer function of the homogeneous medium* $H(f_x, f_y, z_t)$ being defined as

$$H(f_x, f_y, z_t) = \exp[-j2\pi\delta \cdot \left|1/\lambda^2 - f_x^2 - f_y^2\right|^{1/2} \cdot z_t] \tag{8}$$

¶ The FFTW (Fastest Fourier Transform in the West) library can be downloaded at the URL http://www.fftw.org

with $\delta = +1$ for $f_x^2 + f_y^2 \le (1/\lambda)^2$ or $\delta = -j$ for $f_x^2 + f_y^2 > (1/\lambda)^2$ (evanescent wave case). As in the paraxial approximation case of the direct approach, Eq. (7) describes a "plane-to-plane propagation" between two parallel planes Σ_o and Σ_t separated by a distance z_t.

Angular spectrum method in paraxial approximation:

In the paraxial case, the transfer function in Eq. (7) reduces to

$$H(f_x, f_y, z_t) = \exp[-jkz] \cdot \exp[j\pi\lambda z_t \cdot (f_x^2 + f_y^2)] . \tag{9}$$

3.2.3 Gaussian beam decomposition method

The "Gaussian beam decomposition method" has been invented by A. W. Greynolds[3,4], based on ideas of J. A. Arnaud[1]. In contrast to the two "classical" approaches described above, this powerful alternative technique allows to compute a pure wave optical propagation in an "end-to-end" way —without the need for intermediate geometrical optical propagations. The basic idea of the algorithm is to decompose a field distribution at an aperture into a set of spatially confined "fundamental beams" (see Figure 3).

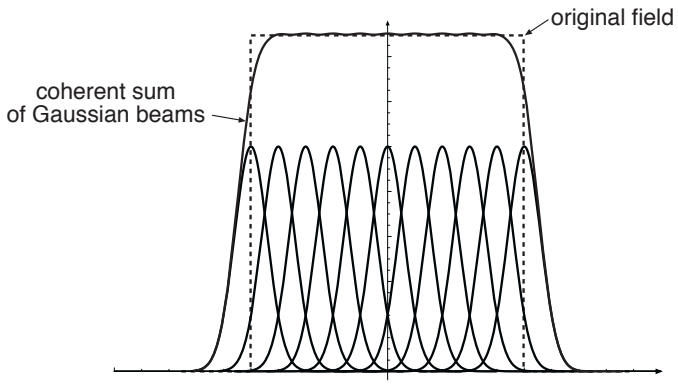

Fig. 3: Principle of decomposing an optical field into a set of Gaussian "fundamental beams"

For calculating the field pattern on any surface of the optical system, the fundamental beams are propagated —including self-diffraction effects— to the surface where they are superposed. The fundamental beam type used in **BeamWarrior** is an astigmatic Gaussian TEM_{00} beam which represents a solution of the paraxial Helmholtz equation (Eq. (4)). Its propagation can be modeled by ray tracing of five rays. The "base ray" defines the main direction of propagation, i.e. the optical axis of the Gaussian beam to which a Jones vector is attached. Four "parabasal" rays (two "waist rays" and two "divergence rays") grouped around the base ray define the self-diffraction of the beam. Figure 4 illustrates the ray-representation of a Gaussian beam whose propagation starts at its beam waist.

The *propagation of an arbitrary optical field* is simulated by decomposing the field into a coherent superposition of equidistantly spaced rotationally symmetric Gaussian beams (waist radii $w_{01} = w_{02} = w_0$ in Figure 4) starting their propagation at their beam waists. For each fundamental beam the four parabasal rays are set up in two orthogonal "astigmatic planes" each holding a waist ray and a divergence ray. The initial divergence angles $\theta_1 = \theta_2 = \text{atan}(\lambda/(4 \cdot w_0))$ are determined by the waist radius w_0. The divergence angle must be small enough, i.e. the initial waist w_0 wide enough, to ensure the validity of the paraxial approximation. The waist should be at least 100 wavelengths wide (e.g. $\lambda = 2\ \mu m \rightarrow w_0 \ge 0.2$ mm). Assuming a minimum number of 10

fundamental beams along one dimension the spatial extension of the field region to be decomposed has to exceed a minimum value of ~1000·λ. However, there exists an alternative way of decomposing a field distribution which is also applicable for spatial extensions below the above mentioned limit: instead of performing the decomposition in the spatial domain it is carried out in the angular spatial frequency domain. A narrow field region is synthesized by a discrete number of fundamental Gaussian beams propagating in different directions, the waist of each beam being wider than the field region to decompose ("directional decomposition"). We intend to add this decomposition technique in a future release of **BeamWarrior**. It is of practical importance when simulating diffraction at narrow pinholes or optical fiber heads.

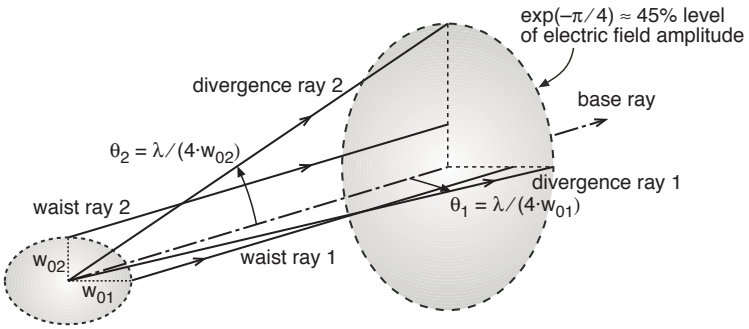

Fig. 4: Representation of an astigmatic Gaussian beam by a base ray and four accompanying parabasal rays. For illustration, the divergence angles are exaggerated.

Each fundamental beam is propagated by tracing its base ray and the four accompanying parabasal rays using the ray tracing algorithm described in Subsection 3.1. Reflection or refraction at optical surfaces is modeled by reflecting or refracting the beam-constituting rays. As a consequence of the ray-based description of the Gaussian beam it has to be made sure that the region of an optical surface sampled by a single beam is locally parabolic or flat. Within the paraxial approximation each beam has a small self-divergence. The angular deviation of its wavefront from a plane is always quite small. Hence, the distinction between the normal to the wavefront and the base ray direction is not significant. The longitudinal component of the electric field vector is negligible. The local Poynting vector direction is equal to the base ray direction. Since the wavefront of each fundamental beam can be considered as plane, the interaction with a reflecting / refracting optical surface can be modeled by applying Fresnel equations, i.e. the Jones formalism used in the polarization ray tracing (Subsection 3.1) can be used.

The *electric field pattern on an arbitrary surface* can be computed from the positions and directions of the base and parabasal rays of the complete set of fundamental beams.[10] If the total beam is clipped by an intermediate aperture placed in the beam train a re-decomposition at the aperture may be necessary. In such a case, the sampling rate of the recreated fundamental beams is adjusted to the spatial structures of the obstruction.

4. COMPARISON OF THE PROPAGATION ALGORITHMS

Following the theoretical description in the previous Section 3, this Section focuses on a more practically oriented summary of pros and cons of the various methods for wave optical propagation.

The ***direct method*** (Subsection 3.2.1) has the disadvantage of relatively long computing times. For a grid of $N \times N$ rays (i.e. Huygens sources) and a $N \times N$ target pixel matrix, the complexity of the algorithm scales as $\sim N^4$. Since the continuous field distribution on Σ_o is sampled at a discrete spatial frequency the calculated dif-

fraction pattern on Σ_t repeats itself in space. Aliasing effects arise in case of too low sampling rates on Σ_o. The method has the advantage to be very accurate except for very small propagation distances. It is applicable to problems with complex and / or skew geometries without requiring a specific coordinate system or the usage of "reference surfaces" to sample the beam. The pixel grid on the target surface Σ_t can be flexibly chosen allowing a high spatial resolution in the computed field. Due to its high accuracy, a typical application is cross-checking a result obtained by another algorithm.

Employing an FFT, the ***direct method in paraxial approximation*** (Subsection 3.2.1) provides a significant increase in computational efficiency. For a pixel grid size of $N \times N$ the algorithm has a complexity of $\sim N^2 \cdot \log_2 N$. As a consequence of the FFT the pixel sizes on object and target surface Σ_o and Σ_t are linked to each other, i.e. they cannot be chosen independently. For a square grid the relation linking the object pixel size Δx_o to the image pixel size Δx_t is: $\Delta x_o \cdot \Delta x_t = \lambda z_t / N$. To improve the spatial resolution on Σ_t columns and lines of zeros are added to the pixel matrix on Σ_o ("zero padding"). Two requirements must be met by the pixel size Δx_o: To avoid aliasing errors in the target field distribution Δx_o has to be small enough to ensure that no significant fraction of the diffracted energy is located at spatial frequencies beyond the maximum value $f_x = 1/(2\Delta x_o)$ captured by the FFT. Second, Δx_o must be small enough to capture phase variations of the field on Σ_o corresponding to one wavelength. For meaningful results there should be at least a few samples per phase change of 2π. A value of 5 samples has proven to be sensible in practice. Therefore it is desirable that the phasefronts of the propagating wave are well aligned to the planes Σ_o and Σ_t. Being more efficient and less flexible than the direct method, this approach is well suited to model the propagation of an almost collimated beam over a large distance.

With and without paraxial approximation the ***angular spectrum method*** (Subsection 3.2.2) has the computational cost of two FFTs, hence a complexity of $\sim 2N^2 \cdot \log_2 N$ for a square $N \times N$ grid. The object and target pixel sizes are equal, $\Delta x_o = \Delta x_t$ which is useful for near-field problems and is a drawback in the far-field case (where one is typically interested in having a large Δx_t and a much smaller Δx_o). Requirements in terms of zero padding and prevention of aliasing are similar to those for the direct method in paraxial approximation. The paraxial approximations of the angular spectrum method (Eq. (7) with Eq. (9)) and the direct method (Eq. (5)) are mathematically equivalent. Both are exact solutions of the paraxial Helmholtz equation (Eq. (4)). However, they differ with respect to their numerical behavior. The oscillating quadratic phase factor in the direct paraxial solution Eq. (5) is proportional to the Fresnel number $N_F = A/\lambda z_t$ leading to a decrease in accuracy for large values of N_F, i.e. in the near-field. In contrast, the transfer function Eq. (9) in the angular spectrum paraxial solution Eq. (7) becomes more oscillatory for small N_F values, hence this solution is less accurate in the far-field. A criterion to decide which method is preferable according to computational efficiency and accuracy has been derived by *Mendlovic et al. 1997*[5]: A critical distance is given by $z_c = (2A^{1/2} \cdot \delta)/\lambda$ with the initial beam area A (unit m^2) and the object's finest detail δ (unit m). For distances $z < z_c$ the angular spectrum approach should be used whereas for distances $z > z_c$ the direct paraxial method is more adequate.

The ***Gaussian beam decomposition technique*** (Subsection 3.2.3) has many advantages over the "classic" approaches discussed above. Based on tracing rays ("beam tracing") it is the only wave optical algorithm capable of accurately modeling an "end-to-end" propagation through an optical system. Using the direct or angular spectrum methods, such an "end-to-end" propagation is only possible by combining the wave-optical propagations with intermediate geometrical optical propagations within a "hybrid propagation model".[7] The hybrid model allows to reconstruct a ray triangle grid (compare Subsection 3.1) on the basis of an electric field pattern resulting from a diffraction propagation. However, this "mixed" approach does not provide sufficient accuracy for imaging applications with a narrow field-of-view, such as the pupil re-imaging process in the VLTI (field of view 200 arcsec ≈ 1.e–03 rad).

Because it does not rely on discrete sampling of the initial field rather than synthesis of the field by continuous fundamental beams, the Gaussian beam decomposition technique does not suffer from aliasing problems. Similar as in the direct method, the target pixel size can be chosen freely. Due to the finite spatial extent of a Gaussian beam the number of pixels on the target surface receiving a significant field contribution is generally lower than the total number of pixels where the field is to be computed. A quick pre-selection of the "illuminated" pixel region for each fundamental beam provides a high computational efficiency, especially in near-field computations. The efficiency inversely scales with the "amount of diffraction" present in the field, i.e. the required time for computing the field pattern at a (intermediate / exit) pupil plane is much shorter than the time required for computing the field pattern at an image plane.

Since for each fundamental beam the integrated optical path is known, temporal coherence effects due to a finite bandwidth $\Delta\lambda << \lambda$ of the radiation can easily be taken into account during field computation. By incoherently combining several spectral bands, a broadband (polychromatic) partial coherent intensity pattern can be computed.

The accuracy of the decomposition technique heavily depends on the sampling quality in the object surface, i.e. the number of fundamental beams, their waist size(s) and the distances between the individual beam centers. Questions and tradeoffs related to the decomposition are discussed in reference[3].

5. SUMMARY AND FUTURE WORK

Aiming at the generation of optical models to be integrated into dynamic simulations of controlled optomechanical systems, the modeling tool **BeamWarrior** has been developed. It is part of an "Integrated Modeling Toolbox" described in *Wilhelm, Koehler et al. 2002* (these proceedings).[11] Light propagation is modeled by a set of different algorithms. The geometrical optical domain is covered by a radiometric polarization ray tracing algorithm. Wave optical (diffraction) propagation is handled by three alternative approaches, each being suitable for specific cases: (1) the direct method based on the Rayleigh–Sommerfeld integral, (2) the angular spectrum method using a decomposition of the optical field into a set of homogeneous and evanescent plane waves, and (3) the powerful Gaussian beam decomposition technique which allows to simulate an "end-to-end" wave optical propagation. All algorithms consider polarization effects and are radiometrically calibrated.

Following a theoretical description of the propagation algorithms, the article discusses pros and cons of the different methods with regard to their application in practice. A main future objective is the extension of the Gaussian beam decomposition algorithm towards a "directional decomposition scheme" which is required to model diffraction at fine structures as mentioned in Subsection 3.2.3.

REFERENCES

1. J. A. Arnaud, "Nonorthogonal Optical Waveguides and Resonators", *Bell System Technical Journal*, **Nov. 1970**, p. 2311, 1970
2. J. W. Goodman, *Introduction to Fourier Optics*, McGraw-Hill Publishing Company, New York, 1968
3. A. Greynolds, "Propagation of general astigmatic Gaussian beams along skew ray paths", *Diffractive Phenomena in Optical Engineering Applications*, Proc. SPIE Vol. **560**, pp. 33–50, 1985
4. A. Greynolds, "Vector-formulation of ray-equivalent method for general Gaussian beam propagation", *Current Developments in Optical Engineering and Diffractive Phenomena*, Proc. SPIE Vol. **679**, pp. 129–133, 1986

5. D. Mendlovic, Z. Zalevsky, N. Konforti, “Computation considerations and fast algorithms for calculating the diffraction integral”, *Journal of Modern Optics*, Vol. **44**, No. 2, pp. 407–414, 1997
6. D. C. Redding, W. G. Breckenridge, “Optical Modeling for Dynamics and Control Analysis”, *Journal of Guidance, Control and Dynamics*, Vol. **14**, No. 5, pp. 1021–1032, 1991
7. R. Wilhelm, U. Johann, “Novel approach to dynamic modeling of active optical instruments”, *Design and Engineering of Optical Systems II*, F. Merkle, Ed., Proc. SPIE Vol. **3737**, pp. 45–56, 1999
8. R. Wilhelm, B. Koehler, “Modular toolbox for dynamic simulation of astronomical telescopes and its application to the VLTI”, *Interferometry in Optical Astronomy*, Proc. SPIE, Vol. **4006**, Part One, pp. 124–135, 2000
9. R. Wilhelm, *Novel numerical model for dynamic simulation of optical stellar interferometers*, Logos Verlag Berlin, 2000, also: Technische Universität Berlin, Dissertation, 2000
10. R. Wilhelm, “Comparing geometrical and wave optical algorithms of a novel propagation code applied to the VLTI”, *Wave-Optical Systems Engineering*, F. Wyrowski, Ed., Proc. SPIE Vol. **4436**, pp. 89–100 (2001)
11. R. Wilhelm, B. Koehler, et al. “Integrated modeling for stellar interferometry —motivation, development strategy and practical usage”, *Integrated Modeling of Telescopes*, these proceedings, 2002